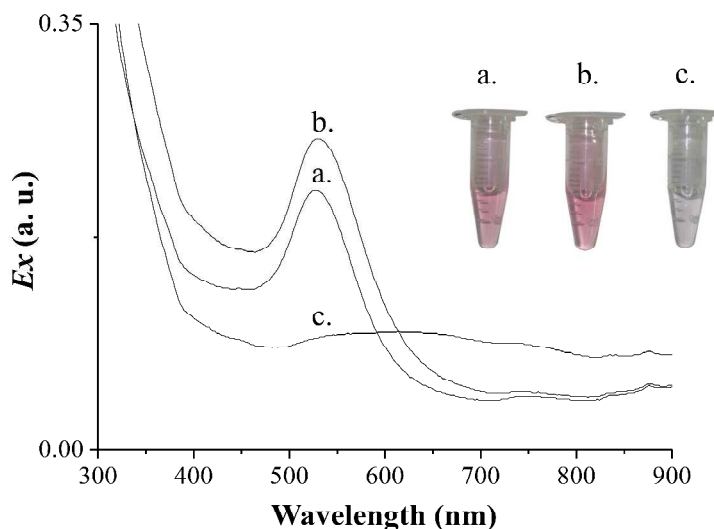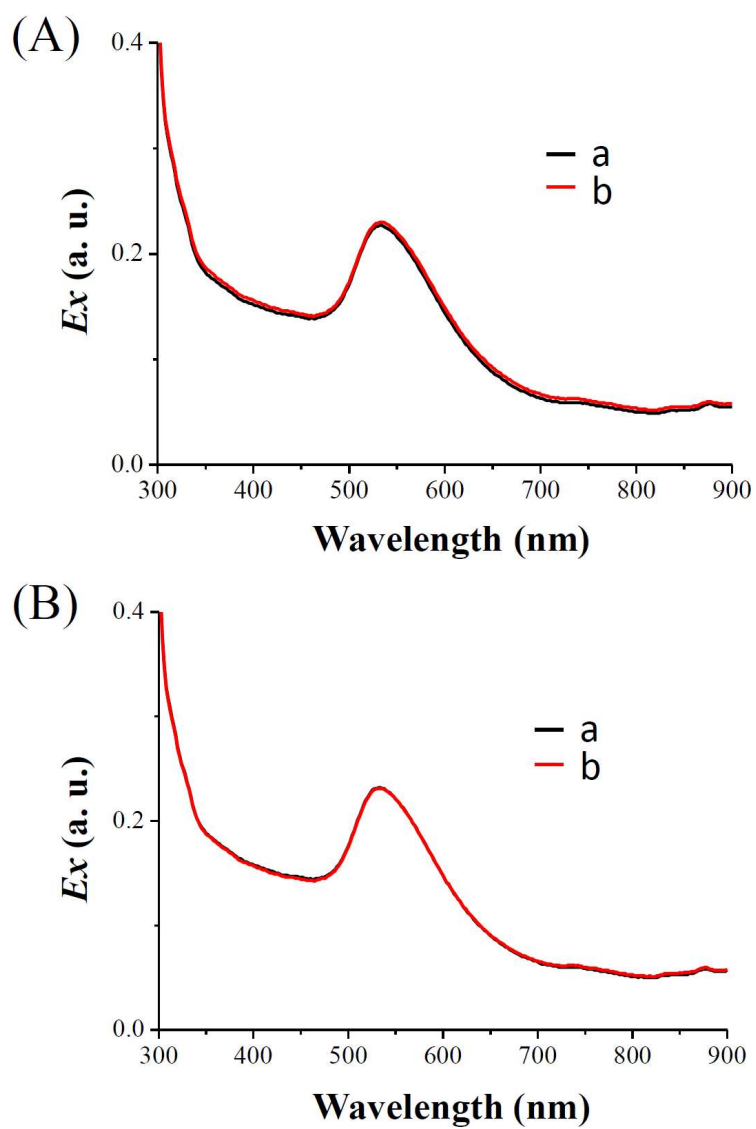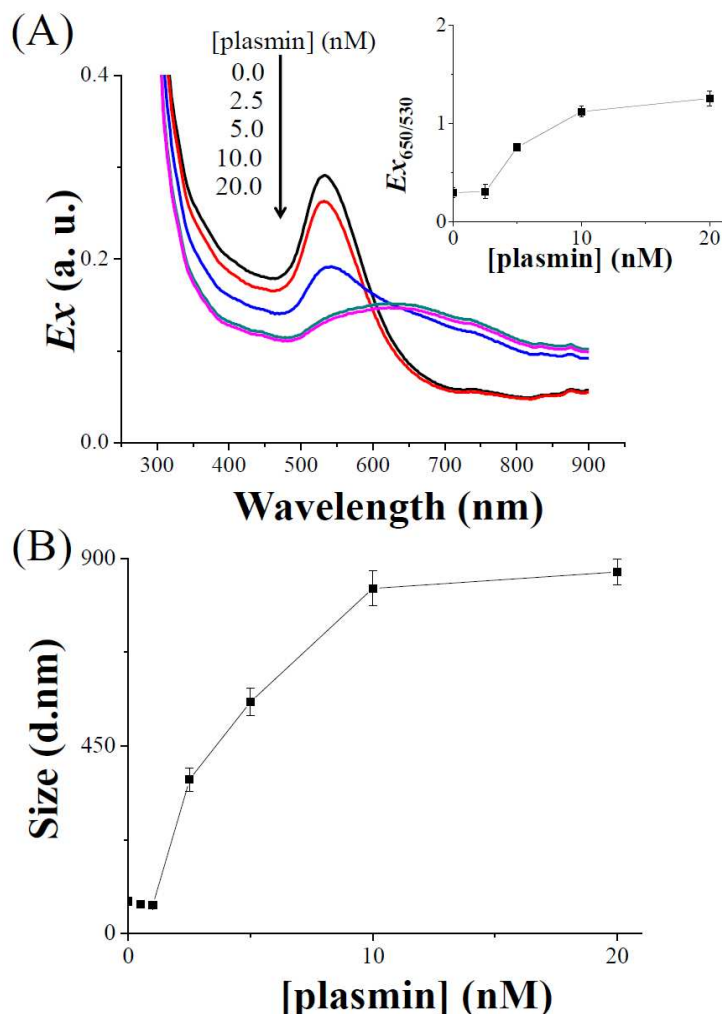**Figure S1.** UV–Vis absorption spectra of 0.2X physiological buffer containing 100 µM BSA and (a) 32-nm Au NPs (100 pM), (b) a mixture of Fib (20 nM) and 32-nm Au NPs (100 pM) that had been incubated for 30 min, and (c) a mixture of Fib (20 nM) and 32-nm Au NPs (100 pM) that had been incubated for 30 min and then reacted with plasmin (10 nM; ca. 4.3×10^{-3} unit/mL; one unit will produce 1 µmol of p-nitroanilide from D-Val–Leu–Lys–p-nitroanilide per minute at pH 7.5 at 37 °C) for 1 h. Inset: photographs of the Au NP and Fib–Au NPs solutions. The extinction (*Ex*) of Au NPs and Fib–Au NPs is plotted in arbitrary units (a. u.).
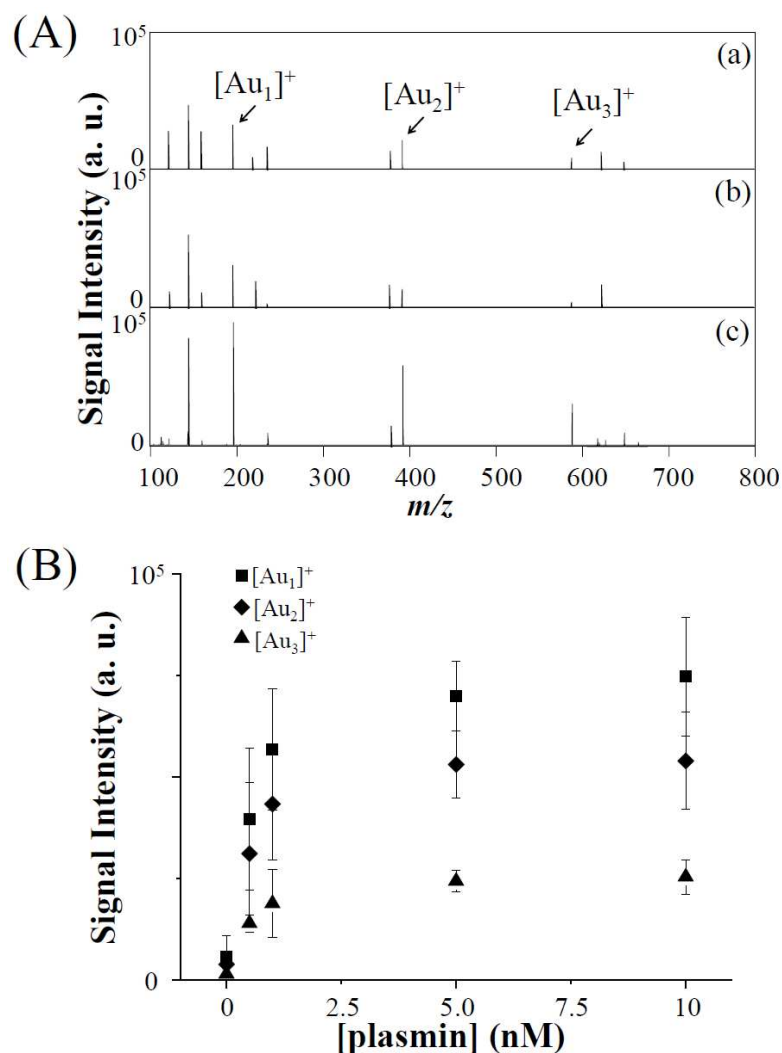
(A)

(B)

Figure S2. UV−Vis absorption spectra of (A) BSA−Au NPs in the (a) absence and (b) presence of plasmin and (B) Fib−Au NPs in the (a) absence and (b) presence of plasminogen (10 nM) in 0.2X physiological buffer, respectively. Other conditions were the same as those described in Figure S1.

Figure S3. (A) UV–Vis absorption spectra and (B) hydrodynamic sizes of Fib–Au NPs (100 pM) in 0.2X physiological buffer containing 100 µM BSA in the presence of plasmin (0–20.0 nM). Inset to (A): Values of $Ex_{650/530}$ plotted with respect to the plasmin concentration. Error bars in the inset are standard deviations across four repeated experiments. Other conditions were the same as those described in Figure S1.

The dispersed Au NPs (32 nm) displayed an extinction band at 530 nm; upon aggregation, the signal underwent a red-shift with decreased extinction, while the intensity of the signal at 650 nm increased. Thus, the bands at 650 and 530 nm were related to the quantities of the aggregated and dispersed Au NPs, respectively. The extinction ratio ($Ex_{650/530}$) could, therefore, be used as a measure of the degree of aggregation, with high values corresponding to high degrees of aggregation.

Figure S4. (A) Mass spectra of (a) Au NPs and (b, c) Fib–Au NPs in the (b) absence and (c) presence of plasmin (10 nM). (B) Signal intensities of the $[Au_1]^+$, $[Au_2]^+$, and $[Au_3]^+$ ions plotted with respect to the concentration of plasmin (0–10 nM). Prior to SALDI-TOF MS measurements, an aliquot (2 µL) of the Au NP or Fib–Au NP samples was cast onto a stainless-steel, 384-well target plate and dried in air at room temperature. Other conditions were the same as those described in Figure S1.
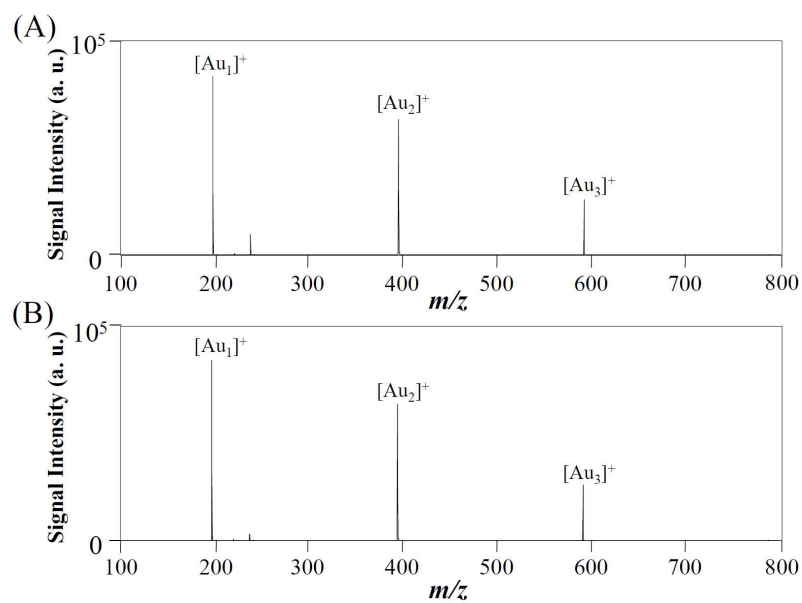
Figure S5. Mass spectra of the BSA−Au NPs/MCEM in the (A) absence and (B) presence of plasmin (10 nM). The peaks at *m/z* 196.967, 393.933, and 590.900 represent the $[Au_1]^+$, $[Au_2]^+$, and $[Au_3]^+$ ions, respectively. Other conditions were the same as those described in Figure 1.
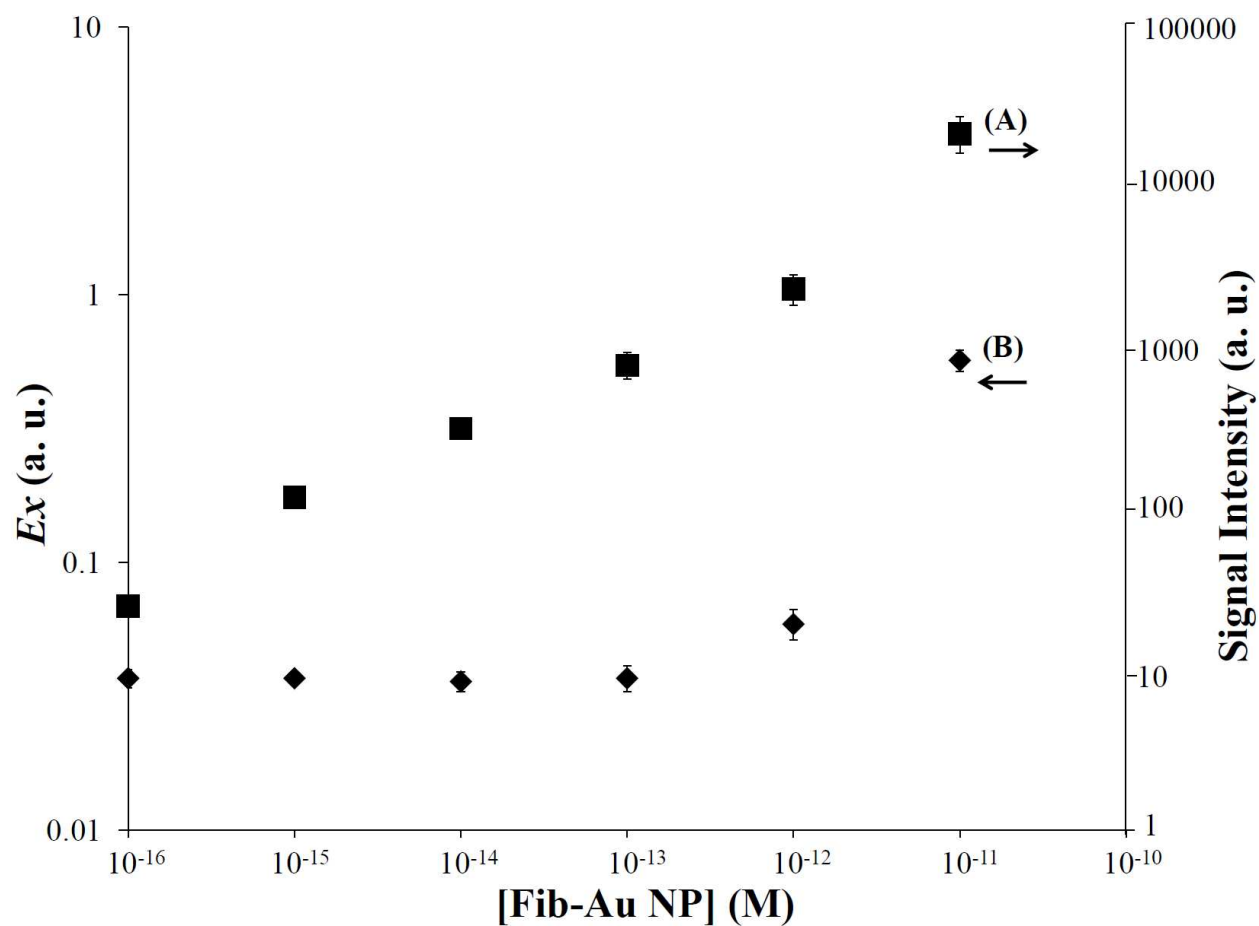
Figure S6. (A) Signal intensities of $[Au_1]^+$ ions recorded through LDI-MS from a Fib–Au NP/MCEM substrate after the MCEM had been immersed in Fib–Au NP solutions of various concentrations (0.1 fM–100 pM). (B) UV−Vis absorptions at 530 nm (SPR band) of Fib–Au NPs at concentrations from 0.1 fM to 100 pM.
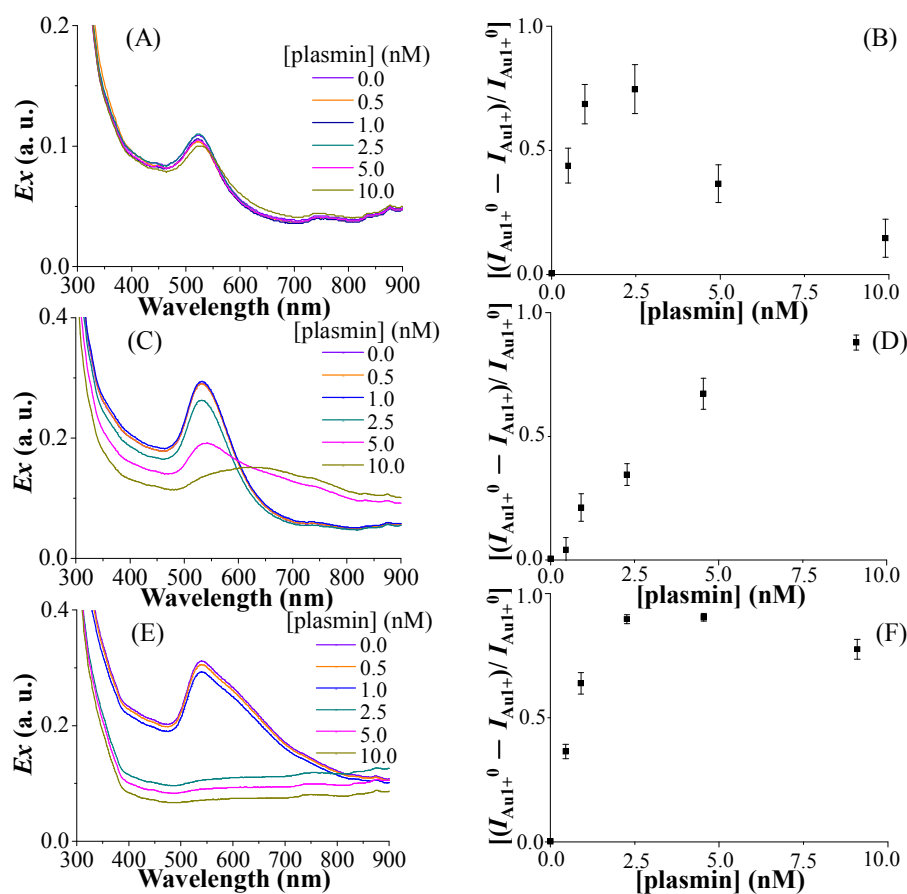
Figure S7. (A, C, E) Colorimetric and (B, D, F) LDI-MS analyses of plasmin using the (A, C, E) Fib–Au NPs and (B, D, F) Fib–Au NP/MCEM substrate as matrices. The sizes of the Au NPs in A and B, C and D, and E and F were 13, 32, and 56 nm, respectively. (B, D, F) Recorded relative signal intensities of the $[Au_1]^+$ ions $[(I_{Au1+}^0 - I_{Au1+})/I_{Au1+}^0]$ in the absence (I_{Au1+}^0) and presence (I_{Au1+}) of plasmin.